

A System Concept for the Advanced Post-TRMM Rainfall Profiling Radars

Eastwood Im

Jet Propulsion Laboratory
4800 Oak Grove Drive, Pasadena, CA 91109, USA
and

Eric A. Smith

Department of Meteorology, Florida State University
Tallahassee, FL 32306-4520, USA

1. Introduction

Atmospheric latent heating field is fundamental to all modes of atmospheric circulation and upper mixed layer circulations of the ocean. The key to understanding the atmospheric heating process is understanding how and where precipitation occurs. The principal atmospheric processes which link precipitation to atmospheric circulation include: (1) convective mass fluxes in the form of updrafts and downdrafts; (2) microphysical nucleation and growth of hydrometeors; and (3) latent heating through dynamical controls on the gravitation-driven vertical mass flux of precipitation.

It is well-known that surface and near-surface rainfall are two of the key forcing functions on a number of geophysical parameters at the surface-air interface. Over ocean, rainfall variation contributes to the redistribution of water salinity, sea surface temperature, fresh water supply, and marine biology and eco-system. Over land, rainfall plays a significant role in rainforest ecology and chemistry, land hydrology and surface runoff. Precipitation has also been closely linked to a number of atmospheric anomalies and natural hazards that occur at various time scales, including hurricanes, cyclones, tropical depressions, flash floods, droughts, and most noticeable of all, the El Ninos. From this point of view, the significance of global atmospheric precipitation has gone far beyond the science arena - *it has a far-reaching impact on human's socio-economic well-being and sustenance.*

These and many other science applications require the knowledge of, in a global basis, the vertical rain structures, including vertical motion, rain intensity, differentiation of the precipitating hydrometeors' phase state, and the classification of mesoscale physical structure of the rain systems. The only direct means to obtain such information is the use of a spaceborne profiling radar. It is important to mention that the Tropical Rainfall Measuring Mission (TRMM) have made a great stride forward towards this ultimate goal. The Precipitation Radar (PR) aboard the TRMM satellite is the first ever spaceborne radar dedicated to three-dimensional, global precipitation measurements over the tropics and the subtropics, as well as the detailed synopsis of a wide range of tropical rain storm systems. In only twelve months since launch, the PR, together with other science instruments aboard the satellite have already provided unprecedented insights into the rainfall systems. It is anticipated that a lot more exciting and important rain observations would be made by TRMM throughout its mission duration.

While TRMM has provided invaluable data to the user community, it is only the first step towards advancing our knowledge on rain processes and its contributions to climate variability. It is envisioned that a TRMM follow-on mission is needed in such a way to capitalize on the pioneering information provided by TRMM, and its instrument capability must be extended beyond TRMM in such a way to fully address the key science questions from microphysical to climatic time scale. In fact, a number of new and innovative mission concepts have recently put forth for this purpose. Almost all of these new concepts have suggested the utility of a more advanced, high-resolution, Doppler-enabled, vertical profiling radar that can provide multi-parameter observations of precipitation. In this paper, a system concept for a second-generation precipitation radar (PR-2) which addresses the above requirements will be described.

2. System Concept

The key PR-2 radar system design concept includes the following capabilities:

- A 13.6/35 GHz dual frequency radar electronics that has Doppler and dual-polarization capabilities.

- A large but light weight, dual-frequency, wide-swath scanning, deployable antenna.
- Digital chirp generation and the corresponding on-board pulse compression scheme. This will allow a significant improvement on rain signal detection without using the traditional, high-peak-power transmitters and without sacrificing the range resolution.
- Radar electronics and algorithm to adaptively scan the antenna so that more time can be spent to observe rain rather than clear air.
- Built-in flexibility on the radar parameters and timing control such that the same radar can be used by different future rain missions. This will help to reduce the overall instrument development costs.

Dual-frequency radar: The TRMM radar operates at a 13.8-GHz center frequency is less sensitive to the backscattering from smaller raindrops. The PR-2 radar will have both 13.6 and 35 GHz channels to increase the range of measurable rainrates. Specifically, the 35-GHz channel would significantly enhance the light rain and drizzle measurement sensitivity. Furthermore, rainfall rate is governed the raindrop-size distribution (DSD) that involves several parameters, and a dual-frequency system will help to improve the accuracy on the retrieval of rainfall rate. Several dual-frequency radars have been flown on shuttle-borne SAR missions (e.g., Stuhr et al., 1995), although they did not operate at the frequencies of interest. The methodology on implementing a dual-frequency rain radar, therefore, has significant technical heritage.

Large antenna to improve horizontal resolution: One of the major impediments to precipitation retrieval from both radar and radiometer measurements is that non-uniform precipitation coverage within the antenna beam biases the retrieved rainrate profile (e.g., Kozi and Iguchi, 1995). For example, Goldhirsh and Musiani (1986) found that the median size of convective storms off the Virginia coast is about 1.9 km, or a little less than half the nadir footprint of the TRMM radar. To mitigate this problem, rainfall measurements at improved resolution, say 2 km, would be required. This leads to the use of a large (5 to 7 meter diameter) antenna. However, such a large antenna, if it is rigid, cannot be easily accommodated by the typical, low-cost, satellite buses and launch vehicles. In the PR-2 design concept, we will take advantage of the recently emerged technologies on large, light-weight, and deployable antennas.

Doppler velocity: Coherent Doppler techniques are routinely being used by spaceborne synthetic aperture radars (SARs) to correct the spacecraft motions and aliasing with great accuracy (Curlander and McDonough, 1991). In fact, the technique is so successful that it leads to a number of new science applications, including interferometric SARs for detection of solid earth's topography to within a fraction of the radar wavelength (Zebker et al., 1994). Amayenc et al. (1993) have derived a spaceborne Doppler radar concept in which the vertical rain motion within a few degrees from nadir can be determined to ~1 m/s accuracy. Therefore, the acquisition of vertical rain motion measurements to within 1 m/s should not be considered challenging.

Like-polarized and cross-polarized measurements: One of the most significant advances in radar meteorology since the mid-1970s has been the studies of a number of polarimetric techniques for rain retrieval. Among them, the Linear Depolarization Ratio (LDR) technique focuses on the discrimination of the oriented, spherically shaped rain particles from the more randomly oriented, irregularly shaped hydrometeors (e.g., ice and graupel) by their distinct differences in radar polarization signatures (e.g., Kumagai et al., 1993). The examples of the NASA/JPL Airborne Rain Mapping Radar (ARMAR, Durden et al., 1994) collected like-polarized (HH) and cross-polarized (HV) rain profiles as shown in Figure 1 demonstrate the substantial and unique scattering signatures from a mix of hydrometeors at or near the melting level, which otherwise are indistinguishable from the like-pol measurements. The key technical considerations on implementing the dual-polarization capability are: (1) sufficient cross-pol isolation; and (2) sufficient cross-polarized backscatter detection capability since the cross-polarized rain measurements are typically 10 to 12 dB lower than the like-polarized rain measurements.

Pulse compression for rain reflectivity measurement sensitivity improvement: One of the key parameters limiting the full utilization of spaceborne radars for rain mapping is the availability of high peak power transmitters. Since raindrops are much weaker scatterers as compared to solid or ocean surfaces, and therefore, rain mapping demands substantially higher peak power. Furthermore, for reliable detection of the cross-pol rain returns, an even higher peak power level is required. To

remediate this problem, a pulse compression approach is incorporated in the PR-2 design. The pulse compression concept is simple: a long time-duration, frequency-coded pulses containing substantially more energy are transmitted and the radar echoes are compressed such that most of the echo energy is re-focused into the range bins which contain the target returns (rain). For example, the TRMM radar transmits 1.6 micro-sec pulses at the PRF of 2776 Hz (Okamoto et al., 1998). Without changing the TRMM PRF and pulse bandwidth, frequency-coded pulses at 30 micro-sec pulse duration can be used to increase the effective detection sensitivity by 12 dB. Several proven low-sidelobe range compression techniques and technologies (e.g., Tanner et al., 1994) are readily available. The next logical step would be the development of this powerful technique for spaceborne meteorological radar applications.

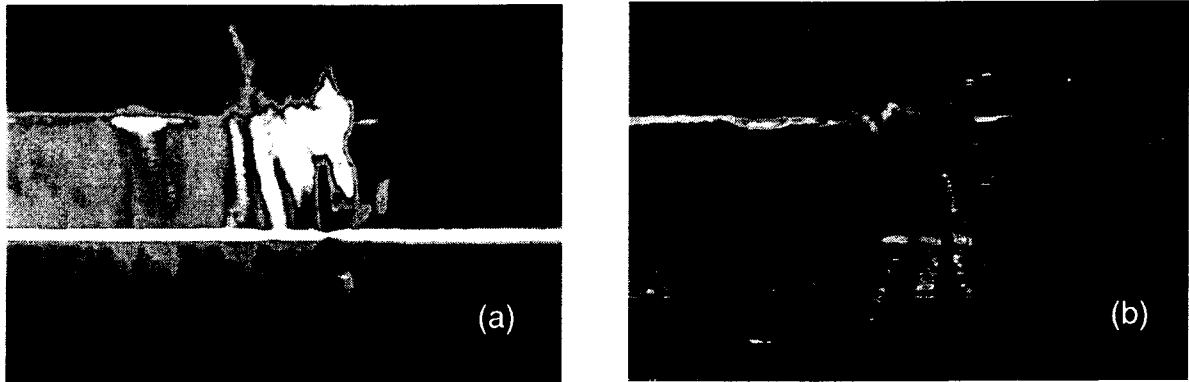


Figure 1: An example of (a) the like-pol and (b) cross-pol radar reflectivity profiles acquired by the NASA/JPL ARMAR during TOGA-COARE.

Ground swath coverage: With the TRMM orbit and its radar swath coverage (~220 km), the sampling frequency at any given point by the TRMM radar is limited to approximately 1 sample every 50 hours (depending somewhat upon the latitude). As such, the TRMM rainfall uncertainties are dominated by the sampling errors. While temporal sampling is an overall mission issue, the spatial sampling can indeed be improved if a radar instrument can provide a wider ground swath. Unfortunately, observation over a large swath means that the time allowed to dwell on any spot on the swath is significantly reduced. As the result, less independent samples would be obtained and the measurement accuracy will suffer. Realizing the fact that rainfall usually occurs over a small fraction of the covered area, the radar observational swath can indeed be increased (without sacrificing the measurement fidelity) by dwelling only on the rain occurring subswath rather than the full swath. This so-called adaptive scan approach is being incorporated into the PR-2 design.

Radar operational and performance robustness: The PR-2 will incorporate a flexible radar timing and pulse parameter design such that it can be re-programmed for use by more than one mission with different orbital and satellite constraints. A similar design was implemented for the radar sensor of the Cassini Mission to Planet Saturn (Im et al., 1993).

3. Design Approach

In order to establish the radar subsystems' requirements and to guide their designs, we have established the following space operation scenarios.

The PR-2 will operate at orbital altitudes (h) ranging between 400 and 750 km, and it will operate in two modes: a Wide-Swath mode in which the antenna will scan $\pm 37^\circ$ across-track at $h=400$ km, and $\pm 28^\circ$ at $h=750$ km. The corresponding ground swaths are 600 and 800 km, respectively. Both the HH-polarized and HV-polarized rain reflectivity profiles at 13.6 and 35 GHz will be measured simultaneously; and a Nadir Doppler mode in which the "vertical" Doppler profiles at nadir will be acquired if precipitation is detected in such regions. The radar antenna size will be 5.3 m at 400 km altitude, and the corresponding horizontal resolution is 2 km at 13.6 GHz. In order to obtain sufficient number of independent samples per resolution cell (TRMM PR obtains 64 samples), the antenna size will be increased only to 7.3 m at 750 km altitude. The corresponding horizontal resolution in this case will be 2.7 km. The horizontal resolution at 35 GHz will be about a factor 3 better. The vertical resolution will be set at 250 m at all altitudes of operation, but the chirp

bandwidth will be 5.3 MHz to allow an 8-fold increase in the number of independent samples. The chirp pulse duration will vary in order to secure sufficient signal-to-noise ratios at all altitudes. The set of PR-2 system parameters are summarized in Table 1.

	h = 400 km		h = 750 km	
	2.73 KHz	2.73 KHz	2.01 KHz	2.01 KHz
Polarization	HH, HV	HH, HV	HH, HV	HH, HV
Antenna effective diameter	5.3 m	2.1 m	7.4 m	2.9 m
Antenna gain	55 dBi	55 dBi	58 dBi	57 dBi
Antenna sidelobe	-30 dB	-30 dB	-30 dB	-30 dB
Polarization isolation	-25 dB	-25 dB	-25 dB	-25 dB
Peak power	200 W	50 W	200 W	50 W
Bandwidth	5.3 MHz	5.3 MHz	5.3 MHz	5.3 MHz
Pulsewidth (wide-swath)	100 usec	100 usec	160 usec	160 usec
Pulsewidth (Doppler)	40 usec	40 usec	40 usec	40 usec
PRF at Wide-swath mode	2.73 KHz	2.73 KHz	2.01 KHz	2.01 KHz
PRF at Doppler mode	5 KHz	5 KHz	5 KHz	5 KHz
Wide-swath dwell time	0.29 sec	0.29 sec	0.39 sec	0.39 sec
Doppler integration time	0.05 sec	0.05 sec	0.05 sec	0.05 sec
Vertical resolution	250 m	250 m	250 m	250 m
Horiz. resolution (nadir)	2 km	2 km	2.7 km	2.7 km
Ground Swath	600 km	600 km	800 km	800 km
Noise-equiv. Zeq (single pulse)	10.0 dBZ	9.8 dBZ	11.7 dBZ	10.6 dBZ
Independent samples	74	74	65	65
Vertical Doppler accuracy	1 m/s	0.9 m/s	1 m/s	0.9 m/s

Table 1: PR-2 radar systems and performance parameters during spaceborne and airborne operations.

Wide Swath Mode: In this mode, rain reflectivity profiles will be measured over a large cross-track swath using the so-called 'adaptive scan' scheme. The designed antenna scan angle range would cover ground swaths ranging between 600 km at 400 km altitude and 800 km at 750 km altitude. As shown in the GATE and other experimental results (e.g., Thiele, ed., 1987), the probability of rain occurrence over a specific location is < 20%. For this reason, and to effectively utilize the limited observation time, each PR-2 observation sequence will be divided into two periods: a Quick-Scan Period to determine the location and vertical extent of the rain cells within the entire swath, and a Dwell Period at which detailed precipitation measurements of the identified rain cells will be made. For example, at $h = 400$ km, a nominal observation sequence will last ~0.29 sec, the Quick-Scan Period will occupy the first 0.09 msec and the Dwell Period will use the remaining available time (0.2 sec). During the Quick-Scan Period the radar system will make a complete cross-track scan through the 600-km swath, transmit and receive only 1 pulse at each 2-km ground resolution cell at a nominal pulse repetition frequency (PRF) of 2730. The radar backscatter measurements at each resolution cell will be averaged on-board over a vertical column of 2 km (~64 samples) and will be compared with a set of thresholds and ranked according to their respective backscatter strength. The ranked results will then be used to develop the subsequent antenna scan pattern for the Dwell Period. In the Dwell Period, the radar will measure the detailed rain backscatter profile over areas with significant rainfall. The nominal swath covered in the Dwell Period is ~200 km, which should be sufficient to cover most of the rain areas within the swath. In the event that there is pervasive rainfall covering areas >200 km cross-track, our proposed dwell pattern would allow observations over cells with the most intense rainfall, thus covering a significant portion of the total rainfall in those areas. On-board processing will include pulse compression and range bin averaging.

Nadir Doppler Mode: When the Quick-Scan results indicate rain occurrence at or near nadir, the Nadir Doppler Mode will be exercised. In this mode, the radar antenna will be pointed at this small region for a total time of ~0.05 sec. A higher pulse repetition frequency (~5000) will be used to accommodate the anticipated Doppler spread. Multiple rain echoes obtained in each resolution cell

will be used to estimate the Doppler shift caused by the mean rainfall motion. This measurement technique is entirely analogous that of Amayenc et al. (1993). The mean vertical rainfall motion can be measured to an accuracy of about 1 m/s.

Detection Sensitivity: Figure 2 shows the signal-to-noise ratios (SNRs) of the like-polarized rain echoes as a function of the rain rate for the PR-2 system. Notice the significant sensitivity improvement, as compared to the TRMM PR, in detecting both very light rain (< 0.1 mm/hr) and very intense rain (~ 90 mm/hr) systems. At rain rates below ~ 15 mm/hr, measurements from both frequencies can be combined to measure the entire rain rate profile. At rain rates between 15 and 35 mm/hr, the dual-frequency measurements can be used to retrieve at least the upper half of the rain clouds. Furthermore, this figure illustrates that there will be sufficient sensitivity for the PR-2 to measure cross-polarized returns at rain rates ≥ 0.2 mm/hr.

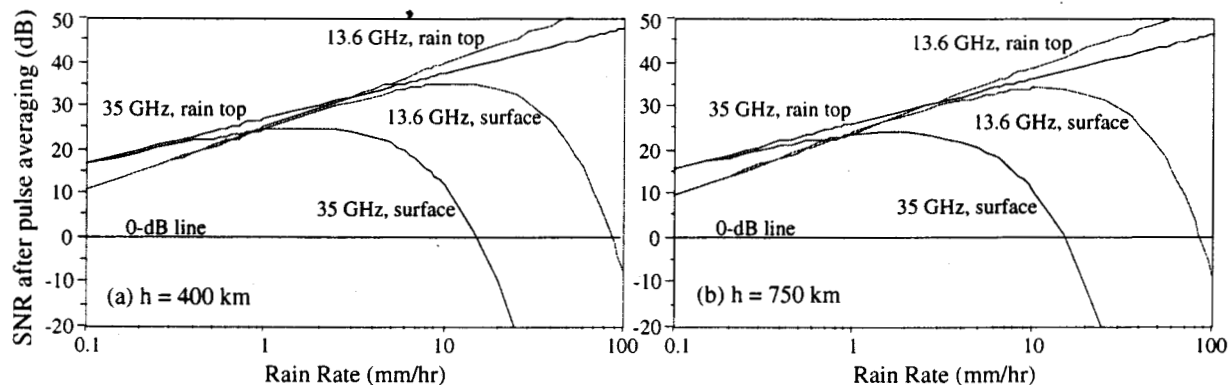


Figure 2: Expected signal-to-noise ratios of the like-polarized rain returns for the PR-2 system and for radar altitudes of: (a) 400 km, and (b) 750 km. The rain top is assumed to be at an altitude of 5 km.

Radar RF electronics subsystem consists of a NCO-based digital chirp generator (DCG) to synthesize the chirp waveform, an upconverter and four receiver channels. The DCG approach, as demonstrated by ARMAR (Tanner et al., 1994) has the benefit of great flexibility in generating the shaped, linearly frequency-modulated pulses with sidelobe levels below -60 dB. The chirp waveform is generated at an IF frequency and upconverted to both Ku-band (13.6 GHz) and Ka-band (35 GHz) using a two-stage mixing process. The LO frequencies are provided by phase-locked oscillators and dielectric resonator oscillators, which are all locked to a reference oscillator for coherent up and downconversion, required for the Doppler mode. The signals are amplified to the desired radiated powers using the 13.6 and 35 GHz traveling wave tube amplifiers (TWTA) and transmitted through an ortho-mode transducer (OMT) and a circulator assembly to the dual-frequency antenna. The OMT and circulator are used to separate the horizontal and vertical polarization components at each frequency. A small amount of power in the transmit pulse is also directly coupled to the receiver channels to calibrate the sensitivity of the system and to accurately measure receiver gain and noise floor, which is essential to achieve the sensitivity and accuracy requirements of the system. There are four receiver channels, two required for 13.6 GHz (H- and V-pol) and two for 35 GHz (H- and V-pol). The receiver amplifies the returned echo using a low noise amplifier and coherently downconverts the signal to offset video.

Digital electronics subsystem includes control and timing unit (CTU), analog-to-digital converters (ADCs) for the four receiver channels, multiplexer, data processor, and data formatter. The control and timing unit decodes all radar mode commands and generates the required timing signals. It also controls the timing of the antenna beam scan. The 14-bit ADCs, with dynamic range greater than 70 dB, digitize the linearly detected video signals. The digitized data is multiplexed and sent to the onboard data processor. The data processor performs pulse compression, range bin averaging, ranking of the data acquired in the Quick-Scan Period to determine the rain regions, and Doppler processing of the data acquired in the Nadir Doppler Period. The processed data are formatted and sent to the tape recorder for storage.

Radar antenna. The large swath coverage and fine horizontal resolution desired for detailed rain profiling by radars lead to the use of a large (5 to 7 m diameter), dual-frequency, scanning antenna. while the TRMM PR type antenna design can be extended to a larger scan range and to two

frequencies, its rigid structure would be too heavy and cannot be easily accommodated by typical, low-cost, satellite buses and launch vehicles. On the other hand, several large, light-weight, and deployable antenna designs have recently emerged and have great potential for adaptation to spaceborne meteorological applications. For example, under JPL's Advanced Radar Technology Program (ARTP), an inflatable L-band SAR array antenna of 10m x 3m is being developed and a shuttle flight demonstration is scheduled for the year of 2000. A reduced-size (3.3m x 1.0m) model of this antenna has already been successfully demonstrated on the ground environment (Huang et al., 1997). It is expected that the full-size antenna will achieve dual-linear-polarization, 80 MHz bandwidth, 52% aperture efficiency, and 60 kg mass ($\sim 2 \text{ kg/m}^2$). Also, a breadboard model of an L/C and L/X-band dual frequency, shared aperture, scanning antenna is currently under development. However, all of them are designed for operations at lower frequencies and are still in the technology demonstration stage. Additional work is required to mitigate the risk and to extend to higher frequencies.

4. Summary

A radar system design for the second-generation spaceborne precipitation radars was presented in this paper. In this design, several innovative features are being incorporated to enhance the rain measurement capability. These include: 13.6/35-GHz dual-frequency operations, a large, shared-aperture, deployable, scanning antenna, dual-polarization, nadir Doppler measurements, pulse compression and real-time data processing, and instrument flexibility. It is anticipated that such instrument concept can provide significant data for advancing our understanding on rain processes, latent heating, climate variability, and atmospheric anomalies.

Acknowledgments

The research described in this paper was performed by the Jet Propulsion Laboratory, California Institute of Technology, under contract with the National Aeronautics and Space Administration.

References

- Amayenc, P., J. Testud, and M. Marzoug, 1993: Proposal for a spaceborne dual-beam rain radar with Doppler capability. *J. Atmos. Oceanic Tech.*, **10**, 262-276.
- Curlander, J.C., and R.N. McDonough, 1991: *Synthetic Aperture Radar - Systems and Signal Processing*. Wiley, 647 pp.
- Durden, S.L., E. Im, F.K. Li, W. Ricketts, A. Tanner, and W. Wilson, 1994: ARMAR: An airborne rain mapping Radar. *J. Atmos. Oceanic Tech.*, **11**, 727-737.
- Goldhirsh J., and B. Musiani, 1986: Rain cell size statistics derived from radar observations at Wallops Island, VA. *IEEE Trans. Geosci. Remote Sensing*, **24**, 947-954.
- Huang, J., M. Lou, and E. Caro, 1997: Super-low-mass spacecraft SAR array concepts. *IEEE AP-S/URSI Symposium*, July 1997, 1288-1291.
- Im, E., W.T.K. Johnson, and S. Hensley, 1993: Cassini Radar for remote sensing of Titan -- design considerations. *IGRSS'93 Symposium*, August 1993.
- Kozu, T., and T. Iguchi, 1995: Non-uniform beam filling correction for spaceborne radar rainfall retrieval. Preprint Vol., 27th AMS Conference on Radar Meteorology [Oct. 9-13; Vail, CO], Amer. Meteor. Soc., Boston, MA, 797-799.
- Kumagai, H., R. Meneghini, and T. Kozu, 1993: Preliminary results from multiparameter airborne rain radar measurement in the western Pacific. *J. Appl. Meteor.*, **32**, 431-440.
- Okamoto, K., T. Iguchi, T. Kozu, H. Kumagai, J. Awaka, and R. Meneghini, 1998: Early results from the Precipitation Radar on the Tropical Rainfall Measuring Mission. *CLIMPARA'98*, 8 pp.
- Stuhr, F., R. Jordan, and M. Werner, 1995: SIR-C/X-SAR: A multifaceted radar. *IEEE AES Systems*, **10**, 15-24.
- Tanner, A., S.L. Durden, R. Denning, E. Im, F.K. Li, W. Ricketts, and W. Wilson, 1994: Pulse compression with very low sidelobes in an airborne rain mapping radar. *IEEE Geo. Sci. & Remote Sens.*, **32**, 211-213.
- Thiele, O. W., ed., 1987: On requirements for a satellite mission to measure tropical rainfall. NASA Ref. Pub. 1183.
- Zebker, H.A., C.L. Werner, P.A. Rosen, and S. Hensley, 1994: Accuracy of topographic maps derived from ERS-1 interferometric radar. *IEEE Geo. Sci. & Remote Sens.*, **32**, 823-836.